

# New Approaches to the Modelling of Lake Basin Morphometry

Håkan Johansson · A. Angelica Brolin · Lars Håkanson

Received: 23 August 2004 / Accepted: 10 August 2006 / Published online: 19 January 2007  
© Springer Science + Business Media B.V. 2007

**Abstract** In lake modelling, a general and useful method of describing variations in area and volume with depth is of fundamental importance to describe processes and properties that change vertically within a given lake. In this work, two mathematical approaches to describe the shape of a lake basin are introduced and tested against empirical data. The two methods require only three easily available input parameters: maximum depth, surface area and volume. The first method is based on a traditional morphometric parameter, the volume development ( $V_d$ ), and the second method on the new hypsographic development parameter ( $H_d$ ). Both methods give area and volume at any depth of a lake and can furthermore be used to estimate lake bottom slopes. Comparisons with empirical area–depth and volume–depth distribution curves from 105 lakes that cover a wide range of lake morphometric characteristics have revealed that the two methods give very satisfactory results. The  $V_d$ -model yields  $r^2$ -values of 0.924 and 0.907 for area and volume description with lake depth, respectively. The corresponding  $r^2$ -values for the  $H_d$ -model are 0.988 and 0.996, respectively. Using the  $H_d$ -model, an approach has also been developed to test when and by how much it is necessary to correct the empirical volume of a lake given the number of measured strata and basin shape.

**Keywords** hypsographic curve · hypsographic development parameter · lake area · morphometry · volume · volume development parameter · water level fluctuations

## 1 Introduction and Aims

Knowledge of the morphological features of a lake is important because the shape of a lake affects nearly all physical, chemical and biological properties in lake ecosystems. The morphology of lakes has, for instance, often been recognised as one of the most important lake characteristics that differentiate the properties of one lake from another (e.g., trophic level, theoretical water retention time, Secchi depth and lake oxygen concentrations). For instance, Rawson [64, 65] and Fee [14] found that mean depth is a dominant factor controlling productivity in lakes and the size of a lake has been shown to be an important factor controlling the depth of the thermocline (e.g., [15, 35, 61]). The shape of a lake also regulates sedimentation, bottom dynamic conditions [21, 68] and concentrations of suspended particulate matter (SPM) [54]. These relationships will be further elaborated in a later section.

To be able to quantitatively describe processes and properties that change vertically in lakes, basic morphometric parameters such as volume, surface area and mean depth do not alone provide the solution. One approach to handle this problem has been to incorporate information related to the hypsographic curves. The hypsographic curve (i.e., the area–depth distribution curve) describes how the area changes with depth in a lake. The hypsographic curve gives information about the two- (2D) and three-dimensional (3D) features of a lake. Based on the hypsographic curve, it is possible to calculate the area and volume at any given water depth, e.g., hypolimnion and epilimnion volumes, and the volume of the photic zone. Similar information is also required in calculations of reservoir volumes with changes in the water level (see e.g., [51, 60]), and fluctuations in water level can be great in lakes in tropical or dry climates [41] and in hydropower dams.

---

H. Johansson · A. A. Brolin (✉) · L. Håkanson  
Department of Earth Sciences, Uppsala University,  
Villavägen 16, SE-752 36 Uppsala, Sweden  
e-mail: Angelica.Brolin@geo.uu.se

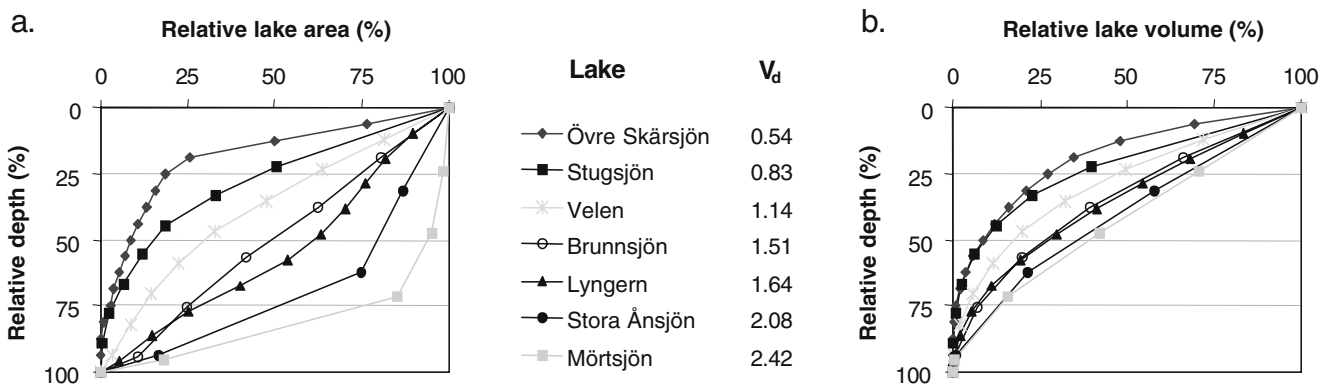


**Fig. 1** The large variability in lake basin shapes as exemplified by lakes with different volume development ( $V_d$ ). (a) Relative area–depth distribution curves. (b) Relative volume–depth distribution curves. (Data from lakes used in this work.)

One way of incorporating the hypsographic curve in lake models has been to fit an equation to either the area–depth distribution curve [42] or the volume–depth distribution curve [11]. A different method was used by James et al. [44], who incorporated an algorithm that uses a look-up table to define depth–volume changes in their lake model. However, these methods to set up specific equations or look-up tables for each new lake are time-consuming and require access to hypsographic curves, which not always are at hand. Another way to derive volumes at different depths would be to use Geographic Information Systems (GIS). This is an area under constant development (e.g., [19, 57]), however, currently there exists no easy ways to link GIS and environmental modelling software [17].

From this background, the aim of this work is to develop a general and useful alternative to lake-specific equations and look-up tables which can be used in lake models to describe how both area and volume changes with depth. In Section 2, the importance of basin shape to lake functions will be illustrated with a few examples. The commonly used approximation for lake volume determinations will then be described, followed by the two new approaches for modelling area–depth and volume–depth relationships. The first approach is based on a traditional morphometric parameter, the volume development ( $V_d$ ). The second approach is based on a new morphometric parameter, the hypsographic development parameter ( $H_d$ ). Both methods require only three easily available input parameters: maximum depth, surface area and volume. The two methods can be used to derive areas and volumes at different depths as well as bottom slope. The new approaches have been tested against empirical data from 105 Swedish lakes. The quality of the data is discussed in Section 2. We then present the results when empirical data are compared to data generated by the two new approaches. We also suggest how to test and correct empirical lake volumes determined with the commonly used volume approximation. Finally, we exemplify the practical use of

the two new approaches for modelling area–depth and volume–depth relationships.

## 2 Motives, Presuppositions and Methodology

Statistical and dynamical models for substances generally include basic lake morphometric parameters such as surface area, volume, mean depth and maximum depth. (For a more thorough description of lake morphometric parameters, see Håkanson [22].) To describe the transport routes and the fate of substances in mass-balance models, there is also a need to correctly describe key controlling parameters such as the inflow concentration of substances [29], the theoretical water retention time of the lakes [27] and particle associations [47]. The morphometric parameters as such are evidently not sufficient to describe many physical, chemical and biological processes and their vertical extensions in lakes. The area–depth distribution curve and the volume–depth distribution curve can provide important complementary information to quantify many lake processes. The hypsographic curves vary among lakes (see Fig. 1). To understand many lake processes, there is a need to mathematically describe how different lake hypsographic curves change with lake depth.

### 2.1 Basin Shape, a Key Parameter Controlling Lake Function

We present a few initial examples to illustrate how important basin shape is for lake functions.

#### 2.1.1 Bottom Dynamic Conditions

In many lakes, wind-induced waves control the bottom dynamic conditions [21, 68]. Induced by the wind speed, wind frequency and fetch (unobstructed distance along a water surface), wave orbitals of moving water induce shear stress on lake bottoms (e.g., [21, 48, 68]). Depending on the

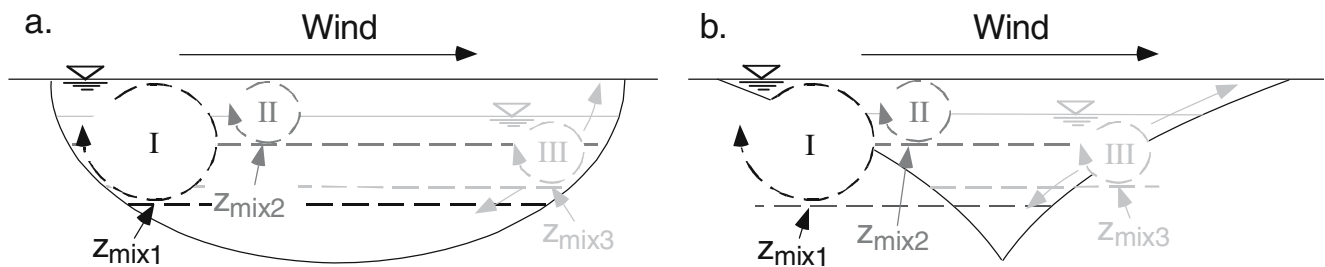


**Fig. 2** Conceptual figure showing how differences in lake form can influence to what extent lakes with identical surface areas and maximum depths will be affected by different vertical processes such as wind-generated mixing. Cases I ( $z_{mix1}$ ) and II ( $z_{mix2}$ ) represent different wind

conditions, whereas case III ( $z_{mix3}$ ) shows an influence of water level fluctuations. (a) Concave lake basin shape ( $V_d > 1$ ). (b) Convex lake basin shape ( $V_d < 1$ )

wind-generated mixing depths and differences in basin shape (see  $z_{mix1}$  and  $z_{mix2}$  in Fig. 2a and b), the bottom areas subjected to high-energy orbitals become larger or smaller (e.g., [24, 25]). In these areas of erosion and transportation, fine-grained particles are redistributed to low-energy accumulation areas (e.g., [21, 68]). In addition to wind/wave action, slopes on bottoms inclining more than 4–5% may induce transportation of bottom sediments (i.e., slope-induced turbidity currents) which additionally modify the bottom conditions [21, 24, 25]. According to Blais and Kalff [4], the accumulation areas in lakes correlate strongly to the mean bottom slopes.

### 2.1.2 Sedimentation, Resuspension and Suspended Particulate Matter

For lakes with identical surface areas, differences in wind conditions and lake form, determine resuspension and hence also variations among lakes in the concentration of SPM [33, 34]. An increase in SPM also elevates the concentration of particle-associated substances such as phosphorus. According to Lindström et al. [54], based on statistical analysis of 26 lakes, differences in lake basin shapes significantly influence the differences in concentration of SPM among lakes. Resuspended particulate material may, in fact, as shown in a study by Weyhenmeyer [72] contribute markedly (47–92%) to the total sedimentation in lakes. The result of Lindström et al. [54] and the interval in resuspension reported by Weyhenmeyer [72] might be explained by the fact that a larger or smaller part of the water column will be subjected to high-energy wave orbitals depending on differences in lake basin shapes, as illustrated in Fig. 2a and b.

### 2.1.3 Sediment Focusing

Sediment focusing is a process where particulate material at the sediment surface are gradually resuspended due to, for instance, wave action, as illustrated in Fig. 2, and focused to deeper areas in lakes (e.g., [4, 33, 40, 43]). The convex lake in Fig. 2 has a large area above the mixing depth, and

the concave one a smaller area exposed. The SPM in the convex lake will be redistributed to a relatively small area. As a result, the convex lake will have a larger sediment focusing factor. Lakes with steep bottom slopes will also have a significant sediment focusing factor, since turbidity currents can redistribute sediment to deeper areas [40]. Differences in sediment focusing among lakes may be explained by differences in bottom slope [4] and in lake basin shape (in terms of different  $V_d$ ) [50].

### 2.1.4 Water Level Fluctuations

A change in the water level not only affects the obvious physical qualities such as the surface area, volume and maximum depth, but also bottom dynamic conditions [31], sedimentation rates [16], resuspension and SPM [31, 59, 69]. An increase in SPM would reduce light penetration [5] and primary production [36, 52, 53]. Figure 2a and b illustrates how a decrease in water level causes the wave base to move downwards and fine sediment erosion to take place in previous accumulation areas. The extent of such changes evidently depends on lake form.

### 2.1.5 Water Retention Time and Active Volume

For stratified lakes with identical surface areas, maximum depths and mixing depths (see Fig. 2a and b), it is the difference in basin shape that determines the proportion of hypolimnetic and epilimnetic volumes. The stability of the thermocline regulates the exchange of water between the epilimnion (the active lake volume) and the hypolimnion and thereby also any replenishment of hypolimnetic water [8, 10]. This influences the seasonal variations in the epilimnetic and hypolimnetic water retention times, which, in turn, have a major impact on retention rates and mass flows of substances in stratified lakes [27]. If the oxygen consumption in the hypolimnion is high, this could lead to fish kill catastrophes and significantly increased diffusion of phosphorus from the bottom sediments [32]. Interestingly, the oxygen consumption rate has been found to vary both with the trophic level as well as with parameters such

as the thickness of the hypolimnetic layer [7], the mean depth [70] and the form of the hypolimnion [9, 56].

### 2.1.6 Littoral Colonisation Zone

The littoral zone has a very high potential for production in most lakes since all major groups of primary producers (phytoplankton, benthic algae and macrophytes) appear in this zone. In shallow lakes, macrophyte production can exceed phytoplankton production [71]. Usually, the littoral zone is defined as the part of the area where the light conditions, or hydrostatic pressure, allows colonisation of macrophytes [39]. For lakes with the same surface area, volume and maximum depth, it is the basin shape that will regulate the extent of the littoral zone. The convex lake in Fig. 2b has a larger littoral zone than the concave lake in Fig. 2a.

### 2.1.7 Lake Productivity

The connection between different morphometric parameters and lake productivity has been addressed in many studies. For example, mean depth is a dominant factor controlling primary production [14] and fish productivity [64, 65]. Kalchew et al. [49] found mean depth to be an important explanatory variable for the total variance of average size of bacterio-, phyto- and zooplankton organisms. Surface area and volume can be used to predict annual fish yield [66] and slope correlates with the submerged macrophyte biomass [12] and the zoobenthic biomass [62] of the littoral zone. Several examples can also be given of how production is affected by factors, which in turn correlate with morphometry. In previous sections, it has been explained how water level fluctuations can affect primary production through increased SPM, how water retention time can affect fish through the oxygen concentration and how the littoral zone can control productivity. A relationship between lake area, mean depth and humic content, which in turn affects lake productivity, has been found by Rasmussen et al. [63]. According to Fee et al. [15], area is the primary determinant of the depth of the mixed layer, which in part determines several factors important to production. Håkanson [30] has successfully predicted changes in biomass of nine key functional groups of organisms, including both primary and secondary producers, with a model based on mean depth, maximum depth and lake area. Håkanson concludes that lake morphometry regulates nutrient concentrations from nutrient loading, and hence also primary production, and consequently secondary production of zooplankton, zoobenthos and fish. Thus, form influences the productivity of lakes.

These examples demonstrate that the structure and function of lakes strongly depend on morphometry. The

mixing depth and the shape of a lake provide a lake-specific distribution coefficient that regulate both the vertical flow of substances and energy as well as the vertical distribution patterns of physical, chemical and biological properties within the lakes.

## 2.2 Area–depth and Volume–depth Relationships and Volume Determinations

From the bathymetric map, several morphometric parameters that represent different features of size and form can be calculated (e.g., volume, lake bottom slope, mean depth and relative depth). Depending on the resolution of the bathymetric map, the volume and associated morphometric parameters will be determined with different accuracy [22]. The volume ( $V$ ) is in the ideal case determined from the integral:

$$V = \int_0^{z_{\max}} A(z) dz \quad (1)$$

where  $z_{\max}$  is the maximum depth (L) and  $A(z)$  is the area–depth function ( $L^2$ ). From echosoundings along transects, one can rarely obtain a continuous area–depth function, so a formula to approximate the volume is generally used. A commonly used approximation is the linear formulation:

$$V = \sum_{j=1}^n \frac{k}{2} (a_j + a_{j-1}) \quad (2)$$

where  $k$  is the contour line interval (L),  $a_j$  is the cumulative area at contour line  $j$  [ $L^2$ ] and  $n$  is the number of contour lines [20]. Håkanson [20] showed that the linear volume calculation formula (equation (2)) can, depending on the shape of the area–depth distribution curve and the number of contour lines with lake depth, cause over- or under-estimations of the true volume.

## 2.3 The New Approaches for Modelling Area–depth and Volume–depth Relationships in Lakes

In the following, we will only use three readily available lake morphometric parameters – surface area, volume and maximum depth – as the basis for the new mathematical functions. The first and simplest approach is to base the function on the volume development ( $V_d$ ), as suggested by Håkanson [28]. The second and more complex approach is presented for the first time in this work. The idea is to find a 3D body whose volume, area and height equals the volume, the surface area and the maximum depth of a given lake. Note that in Section 2.3.1 and Section 2.3.2, both approaches are independent of units (e.g., meters or feet) as long the dimensions are expressed in L for depth,  $L^2$  for area and  $L^3$  for volume.

**Table 1** Classification system for defining the shape of lake hypso-graphic curves and corresponding probabilities, class limits and  $V_d$  values (modified from Håkanson [24])

Lake curve	Label	Probability (%)	Class limits (standard deviations)	$V_d$
Very convex	VCx	6.5	-3 to -1.5	0.05–0.33
Convex	Cx	24.2	-1.5 to -0.5	0.33–0.67
Slightly convex	SCx	38.3	-0.5 to 0.5	0.67–1.0
Linear	L	24.2	0.5 to 1.5	1.0–1.33
Concave	C	6.5	1.5 to 3	1.33–2.0

Data from 48 lakes.

### 2.3.1 Volume Development, and Area and Volume Curves

The idea of the first approach is to derive the requested function from the volume development ( $V_d$ ), a standard, dimensionless morphometric parameter describing lake basin form. Basically,  $V_d$  measures to what degree the volume of a lake deviates from the volume of a cone whose base area and height equals the surface area and the maximum depth.  $V_d = V_{max}/(A_{max}z_{max}/3)$ , where  $V_{max}$  is the volume,  $A_{max}$  is the surface area and  $z_{max}$  is the height of the cone [22]. For  $V_d < 1$ , the lake form is convex, and for  $V_d > 1$  it is concave. This is the classification system for linear, concave and convex lake basin shape used in this work.

The new function presented for the hypsographic curve in this section is derived by finding an equation that describes the lake basin shape probability curves from Håkanson [24] with varying  $V_d$ . These probability curves are based on many empirical hypsographic curves ( $n=48$  lakes) and they describe the probability that a lake should have a linear, convex or concave hypsographic curve (see Table 1). (Note that the lake hypsographic curve classification system presented in Table 1 is not the same as the classification system for linear ( $V_d=1$ ), convex ( $V_d < 1$ ) and concave ( $V_d > 1$ ) lake basin shape used in this paper.) There exists a close relationship between the shape of hypso-graphic curves defined in this way from Gaussian proba-bility curves and the volume development parameter  $V_d$  (see Table 1). While deriving the equation, the following considerations have been made:

- At the shoreline, the new function should be equal to the surface area (i.e., the maximum lake area,  $A_{max}$ ) independent of the lake basin shape, as given by  $V_d$ .
- When the water depth ( $z$ ) is equal to the maximum depth ( $z_{max}$ ), the function should be zero independent of  $V_d$ .
- Between these limits, the function should describe the area [ $A(z)$ ] at any given water depth ( $z$ ).

Using these criteria and the same type of equation as presented by Håkanson [23] to describe characteristic water content of sediments, the model  $A(z) = A_{max} \left[ \frac{z_{max}-z}{z_{max}+z(3-V_d)} \right]^{0.5/V_d}$ ,

where  $A$  is the area,  $A_{max}$  is the surface area,  $z_{max}$  is the maximum depth,  $V_d$  is the volume development parameter [-] and  $z$  is the depth at which the area is calculated, has previously been suggested [28]. After further development, we arrived at the following formula:

$$A(z) = A_{max} [(1 - z_{rel})(1 + z_{rel} \sin \sqrt{z_{rel}})]^{f(V_d)} \tag{3}$$

where  $A$  is the area,  $A_{max}$  is the surface area,  $z$  is the depth at which the area is calculated (from 0 to  $z_{max}$ ),  $z_{rel}$  is the relative depth ( $=z/z_{max}$ ),  $V_d$  is the volume development parameter [-] and  $f(V_d) = 1.7V_d^{-1} + 2.5 - 2.4V_d + 0.23V_d^3$ , which is derived by nonlinear least squares fitting of values from the probability curves from Håkanson [24] to the modelled values.

For the lakes studied in Håkanson [24], one can note that the shape of the mean hypsographic curve is slightly convex (SCx) (see Table 1), and that most lakes are likely to have a hypsographic curve limited by the curves defined by  $\pm 1.5$  SD. Figure 3a shows the shape of these curves in a graphical manner. Figure 3b gives the hypsographic curves calculated by using equation (3) and, for comparison, the previously suggested model. One can note a relatively “good” correspondence between the statistical probability curves and curves calculated using equation (3), especially for all “normal” shapes of the lake hypsographic curves (i.e., class limits -1.5 to 1.5).

Based on equation (3), the volume below depth  $z$ ,  $V(z)$ , can be calculated as:

$$V(z) = \int_{z_i}^{z_{max}} A(z) dz = A_{max} z_{max} \int_{z_{i,rel}}^1 [(1 - z_{rel})(1 + z_{rel} \sin \sqrt{z_{rel}})]^{f(V_d)} dz_{rel} \tag{4}$$

This integral can be approximated by using composite Simpson’s 1/3 rule for four subintervals:

$$\begin{aligned} V(z) &= A_{max} z_{max} \int_{z_{i,rel}}^1 [(1 - z_{rel})(1 + z_{rel} \sin \sqrt{z_{rel}})]^{f(V_d)} dz_{rel} \\ &= \frac{1 - z_{i,rel}}{12} \left[ ((1 - z_{i,rel})(1 + z_{i,rel} \sin \sqrt{z_{i,rel}}))^{f(V_d)} \right. \\ &\quad + 4((0.75 - 0.75z_{i,rel})(1 + (0.25 + 0.75z_{i,rel}) \\ &\quad \left. \sin \sqrt{0.25 + 0.75z_{i,rel}}))^{f(V_d)} \right. \\ &\quad + 2((0.5 - 0.5z_{i,rel})(1 + (0.5 + 0.5z_{i,rel}) \\ &\quad \left. \sin \sqrt{0.5 + 0.5z_{i,rel}}))^{f(V_d)} \right. \\ &\quad + 4((0.25 - 0.25z_{i,rel})(1 + (0.75 + 0.25z_{i,rel}) \\ &\quad \left. \sin \sqrt{0.75 + 0.25z_{i,rel}}))^{f(V_d)} \right] \tag{5} \end{aligned}$$

where  $A_{max}$  is the surface area,  $z_{max}$  is the maximum depth,  $z_i$  is the depth at which the area is calculated (from 0 to

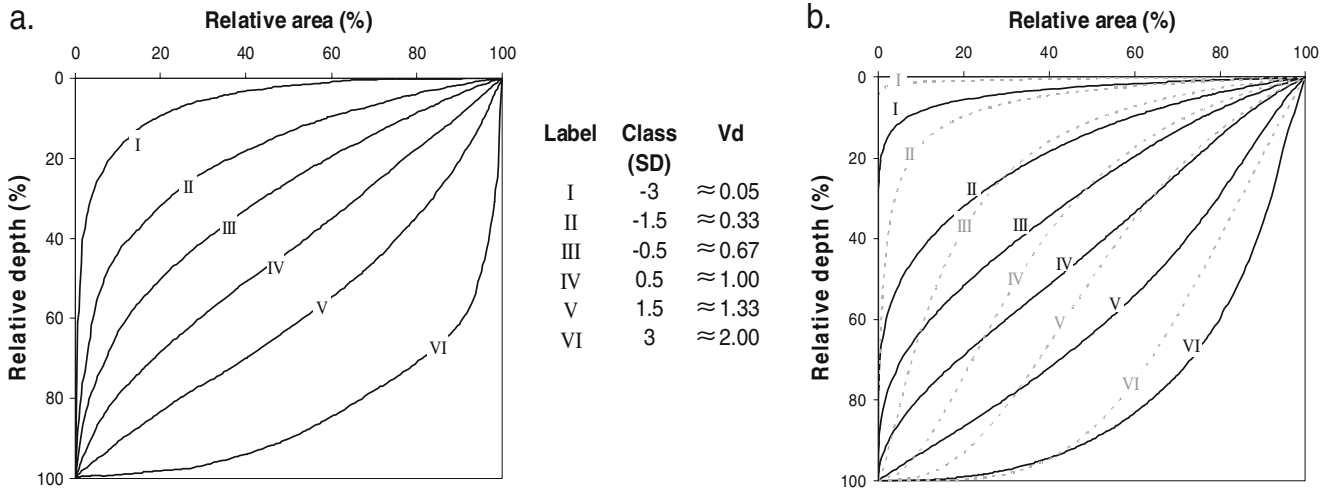


**Fig. 3** (a) Illustration of empirically based statistical probability curves for different lake hypsographic curves and the corresponding  $V_d$ -values (modified from Håkanson [24]). SD = standard deviations.

$z_{max}$ ,  $z_{rel}$  is the relative depth ( $=z/z_{max}$ ),  $V_d$  is the volume development parameter [-] and  $f(V_d) = 1.7V_d^{-1} + 2.5 - 2.4V_d + 0.23V_d^3$ .

Or, by simply assuming that the volume above the depth  $z$  has the average area of  $A_{max}$  and  $A(z)$ , the integral can be approximated as:

$$V(z) = V_{max} - z \left( \frac{A_{max} + A(z)}{2} \right) \tag{6}$$

This is a linear approximation of the area between the two depths (see equation (2)) and it yields an overestimation of the volume when the area–depth distribution curve is concave and an underestimation when it is convex. Note that a partially concave or convex *hypsographic curve* does not necessarily imply that the *basin shape* is concave or convex.

To determine how accurately the Simpson approximation (equation (5)) and the linear approximation (equation (6)) estimate the volume of the generated area–depth distribution curves from equation (3), they have been compared to a third, “more exact”, volume approximation, where the integral in equation (4) was divided into parallelograms with a thickness of 1/1,000 of the maximum depth (i.e., 1 cm thick slices in a lake with a maximum depth of 10 m). The sum of the areas of these parallelograms, from the maximum depth up to  $z$ , then gives the volume of the lake under  $z$ . Comparisons have been made for lakes with  $V_d$  values between 0.05 and 3 with a resolution of 0.05.

Another useful morphometric variable, which can be approximated by using the areas at different depths from equation (3), is the bottom slope. Compared to  $V_d$ , the bottom slope gives more information on the real dimensions of the basin shape. The reason for this is that lakes with identical  $V_d$  do not necessarily have the same slopes since  $V_d$  only expresses the lake form and does not provide any information about the real length scales. The bottom slope,

(b) Illustration of calculated hypsographic curves using the  $V_d$ -approach, equation (3), solid lines and  $A(z) = A_{max} \left[ \frac{z_{max}-z}{z_{max}+zc \left( \frac{z-p+1}{d} \right)^{0.5}} \right]^2$ , dotted lines

on the other hand, includes information about real length scales. The bottom slope in percent is, according to Håkanson [22],  $s=100dy/dx$ , where  $dy$  is change in depth and  $dx$  represents horizontal change. Assuming circular area sections with a radius  $r$  gives the slope at any chosen depth  $z$ :

$$s_1 = 100dz/dr \tag{7}$$

For mathematical reasons, it is not possible to derive  $z(r)$  from equation, (3), i.e.,  $s_1$  can not be calculated in this case. The mean slope ( $s_2$ ) between depths  $z_i$  and  $z_{i+1}$ , on the other hand, can be calculated as:

$$s_2(z_i, z_{i+1}) = 100 \frac{z_i - z_{i+1}}{r_i - r_{i+1}} = 100 \frac{z_i - z_{i+1}}{\sqrt{\frac{A(z_i)}{\pi}} - \sqrt{\frac{A(z_{i+1})}{\pi}}} \tag{8}$$

Note that  $s_2$  is the mean slope of a linear approximation of the area between two depths and not a measure of the mean slope of the *continuous* area–depth distribution curve between the two depths.

### 2.3.2 The Hypsographic Development Parameter and Corresponding Area–depth and Volume–depth Distribution Curves

The aim of the second approach is to find a geometric body whose volume, surface area and the maximum depth should equal a lake. From this, it is necessary that the radius description of the 3D circular geometric body can obtain a non-linear description with depth. This gives the possibility to describe the form of concave or convex geometric bodies.

In a following section, we will show that a lake-specific value for a new parameter, the hypsographic development parameter ( $H_d$ ), will emerge when the empirically determined volume of a lake and the volume of the corresponding geometric body equal each other. The result of this is also a volume–depth distribution function that describes the

geometric 3D body with depth. Since volume–depth and area–depth distribution curves depend on each other, it should also be possible to derive an area–depth distribution function from  $H_d$ .

To obtain identical boundary conditions, it is important that we first normalise the features of the geometric body (i.e., the idealised lake), both vertically and horizontally. It is then possible to postulate a function for the radius description with depth, which only attains values between one and zero. To describe the radius with lake depth,  $r(z)$ , the following expression is given:

$$r(z) = r_{\text{circle}} \left( \frac{H_d^{(-z/z_{\text{max}})} - H_d^{(-z_{\text{max}}/z_{\text{max}})}}{H_d^{(-z_0/z_{\text{max}})} - H_d^{(-z_{\text{max}}/z_{\text{max}})}} \right) \tag{9}$$

where  $r_{\text{circle}} = (A_{\text{max}}/\pi)^{0.5}$  is a scaling factor which equals the radius of a circle with the same area as the lake surface area ( $A_{\text{max}}$ ),  $z$  is the depth,  $z_{\text{max}}$  is the maximum depth,  $z_0$  is the depth at the lake surface from which the depth is measured (i.e.,  $z_0=0$ ),  $A_{\text{max}}$  is the surface area (at  $z_0$ ) and  $H_d$  is the hypsographic development parameter [–]. For any lake-specific  $H_d$ , the area–depth distribution function  $A(z)$  can be determined from:

$$\begin{aligned} A(z) &= \pi(r_{\text{circle}})^2 \left( \frac{H_d^{(-z/z_{\text{max}})} - H_d^{(-z_{\text{max}}/z_{\text{max}})}}{H_d^{(-z_0/z_{\text{max}})} - H_d^{(-z_{\text{max}}/z_{\text{max}})}} \right)^2 \\ &= A_{\text{max}} \left( \frac{H_d^{(-z/z_{\text{max}})} - H_d^{(-z_{\text{max}}/z_{\text{max}})}}{H_d^{(-z_0/z_{\text{max}})} - H_d^{(-z_{\text{max}}/z_{\text{max}})}} \right)^2 \end{aligned} \tag{10}$$

An additional morphometric parameter, which can also be addressed with the  $H_d$  approach, is the bottom slope. The bottom slope can be derived from  $s=100dz/dr$ , where  $r$  is the radius of a circular area section. Depending on whether the aim is to calculate the bottom slope between certain depths or at any chosen depth, the following expressions may be used (multiplication with the factor 100 gives the slopes expressed in percent):

$$\begin{aligned} s_1(z) &= -100 \frac{H_d^{(z/z_{\text{max}}-1)} z_{\text{max}} (H_d - 1)}{r_{\text{circle}} \ln(H_d)} \\ &= -100 \frac{H_d^{(z/z_{\text{max}}-1)} z_{\text{max}} (H_d - 1)}{(A_{\text{max}}/\pi)^{0.5} \ln(H_d)} \end{aligned} \tag{11}$$

$$\begin{aligned} s_2(z_i, z_{i+1}) &= -100 \\ &\times \frac{z_{\text{max}}^2 (1 - H_d^{-1}) (H_d^{(z_{i+1}/z_{\text{max}})} - H_d^{(z_i/z_{\text{max}})})}{r_{\text{circle}} (z_{i+1} - z_i) \ln(H_d)^2} \\ &= -100 \\ &\times \frac{z_{\text{max}}^2 (1 - H_d^{-1}) (H_d^{(z_{i+1}/z_{\text{max}})} - H_d^{(z_i/z_{\text{max}})})}{(A_{\text{max}}/\pi)^{0.5} (z_{i+1} - z_i) \ln(H_d)^2} \end{aligned} \tag{12}$$

where  $s_1$  is the bottom slope in percent at lake depth  $z$  and  $s_2$  is the mean bottom slope in percent between lake depths  $z_i$  and  $z_{i+1}$ , respectively. In comparison to the  $V_d$ -approach, here it was possible to derive an expression for  $s_2$  that gives a measure of the mean slope of the *continuous* area depth distribution curve between two depths.

To facilitate the determination of  $H_d$  for a given lake, we can first derive a general expression to calculate the volume of the 3D geometric body. This can be achieved by recognising that the volume of the 3D geometric body with the radius from equation (9) can be expressed as  $V = \pi \int_0^{z_{\text{max}}} [r(z)]^2 dz$ . The following expression results:

$$\begin{aligned} V(z) &= A_{\text{max}} \int_{z_i}^{z_{i+1}} \left( \frac{H_d^{(-z/z_{\text{max}})} - H_d^{(-z_{\text{max}}/z_{\text{max}})}}{H_d^{(-z_0/z_{\text{max}})} - H_d^{(-z_{\text{max}}/z_{\text{max}})}} \right)^2 dz \\ &= \frac{A_{\text{max}}}{(1 - H_d^{-1})^2} \left[ \frac{2z_{\text{max}} H_d^{(-z/z_{\text{max}}-1)}}{\ln(H_d)} \right. \\ &\quad \left. - \frac{z_{\text{max}} H_d^{(-2z/z_{\text{max}})}}{2 \ln(H_d)} + H_d^{-2z} \right]_{z_i}^{z_{i+1}} \end{aligned} \tag{13}$$

where  $V(z)$  is the volume–depth distribution function. By means of numerical iterations, lake-specific  $H_d$  values can be found for any lake with a known volume ( $V_{\text{max}}$ ), surface area ( $A_{\text{max}}$ ), maximum depth ( $z_{\text{max}}$ ) and where  $z_i$  and  $z_{i+1}$  equals  $z_0$  and  $z_{\text{max}}$ , respectively. Since  $V_d = (3V_{\text{max}})/(A_{\text{max}}z_{\text{max}})$ , we can further substitute  $V(z)$  in equation (13) with  $(V_d A_{\text{max}} z_{\text{max}})/3$ . The resulting function, equation (14), however, cannot be solved analytically for  $H_d$ :

$$V_d = 3 \left( \frac{3 + H_d^2 - 4H_d + 2 \ln(H_d)}{2 \ln(H_d)(H_d - 1)^2} \right) \tag{14}$$

An illustration of the relationship between  $H_d$  and  $V_d$  from a numerical solution of equation (14) is given in Fig. 4. Solving equation (14) numerically is both time-consuming and impractical. By means of statistical methods such as regressions, it is, however, possible to find practical equations that can be used to recalculate  $V_d$  into  $H_d$  with an acceptable accuracy. The allowed maximum deviation in percent, between numerically determined  $H_d$  from equation (14) and estimated  $H_d$  from  $V_d$ , calculated as  $100|H_{d,\text{numerical}} - H_{d,\text{estimated}}|/H_{d,\text{numerical}}$ , was set to  $\pm 0.55\%$  during this procedure. Note that no solution exists for any of the derived equations (9)–(14) when  $H_d=0$  or  $H_d=1$ . When  $H_d=1$  (implies that  $V_d=1$ , see Fig. 4), the lake geometrically takes the shape of a cone and the volume expression for a cone can be used.

$V_d$ -values below 0.33 or above 2.70 seem to be very unlikely, see Fig. 5, or Neumann’s study [58], including over 100 lakes, or from our morphological database with 398 additional lakes. This explains why equations that can be used for recalculations of  $V_d$ -values outside of this range

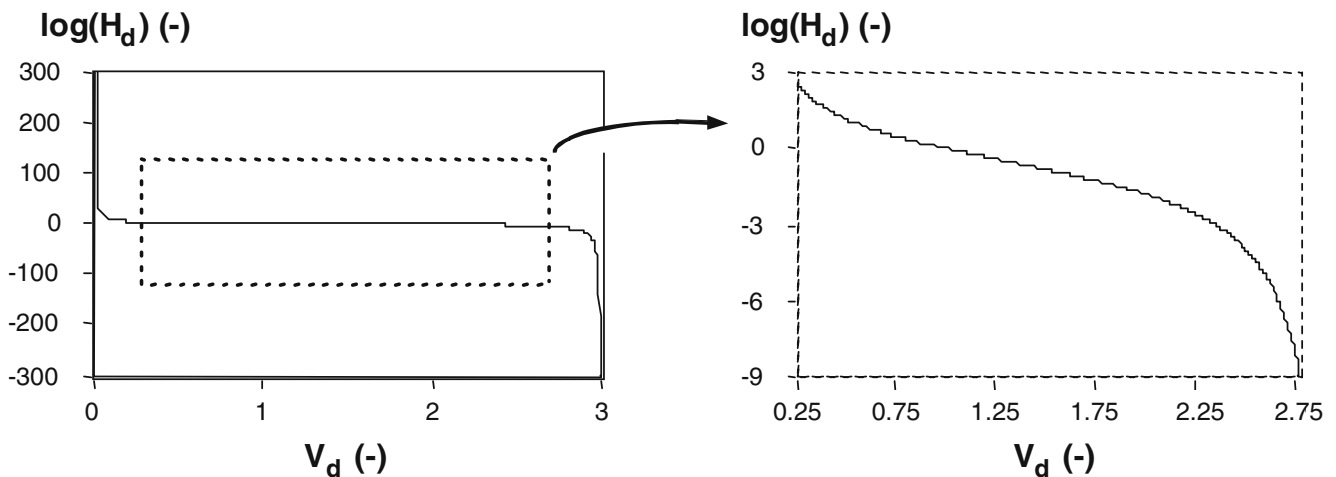


**Fig. 4** Numerically determined  $H_d$  for different idealised lake basin shapes, and its correlation with  $V_d$ . Correlation for the whole  $V_d$ -definable range (see solid frame), whereas dashed frame visualises the  $V_d$ -range, which most likely covers the main portion of lakes in the world

have not been derived. To estimate  $H_d$  from  $V_d$ , the following equations may then be used:

$$H_d(b) = 10^{(1.6b^4 - 2.1b^3 - 1.2b^2 - 3.92b)} \quad (0.20 \leq V_d \leq 0.55) \quad (15)$$

$$H_d(b) = 10^{(-34b^5 - 18b^4 - 6.3b^3 - 1.9b^2 - 4b)} \quad (0.55 \leq V_d \leq 1.85) \quad (16)$$

$$H_d(b) = 10^{(-19261b^5 + 27179b^4 - 15506b^3 + 4432.6b^2 - 639.51b + 36.442)} \quad (1.85 \leq V_d \leq 2.40) \quad (17)$$

$$H_d(b) = 10^{(-3077645b^5 + 6028981b^4 - 4728714.5b^3 + 1855729.6b^2 - 364329.44b + 28621.94)} \quad (2.40 \leq V_d \leq 2.70) \quad (18)$$

where  $b = \log(V_d)$  [-]. Thus, based on equations (15)–(18),  $H_d$  may be determined from the much more easily determined  $V_d$  value with an accuracy of  $\pm 0.55\%$ . The accuracy of the recalculation procedure, however, depends on the given number of digits for the  $V_d$  value. To minimise this dependency,  $V_d$  should be given with at least two decimal digits.

### 3 Lake Morphometric Database

The empirical data originates from a number of Swedish lake studies. The lakes are distributed approximately from  $56^\circ$  to  $68^\circ\text{N}$  (lat.) and from  $1^\circ$  to  $22^\circ\text{E}$  (long.) and they

cover an area of about  $400,000 \text{ km}^2$ . Most of the lakes belong to the in Sweden [26] and worldwide [55] predominating glacial lakes.

#### 3.1 Lake Bathymetric Data Quality Selection Criteria

Depending on the lake form and the number of contour lines in bathymetric maps, the empirical volume may be more or less accurately determined using the linear volume calculation formula (Section 2.2). To compare empirical area–depth and volume–depth distribution curves and modelled ones, it is necessary to remit lakes with unacceptably large errors in the volume determination from the lake database. To select lakes with an error less than  $\pm 2\%$  in the empirical volume, we compared the volumes of idealised area–depth distribution curves with volume estimations made with the linear volume calculation formula (equation (2)). The idealised area–depth distribution curves were generated from  $H_d$  (equation (10)). This procedure was carried out for different basin shapes ( $V_d = 0.05$ – $3$ ) and different numbers of equidistant strata ( $n = 2$ – $100$ ). In this way, it was possible to determine how large the probable error would be given a certain number of strata in a lake and a certain basin shape ( $V_d$ ). From this, it was then possible to identify and remove lakes that probably yield larger volume errors than  $\pm 2\%$ .

#### 3.2 Lake Database for Comparisons of Area–depth and Volume–depth Distribution Curves

Based on the criterion that each hypsographic curve should yield a volume error less than  $\pm 2\%$ , we removed 18 lakes from the original database, leaving 105 lakes for further analyses. The selected lakes and their characteristics are



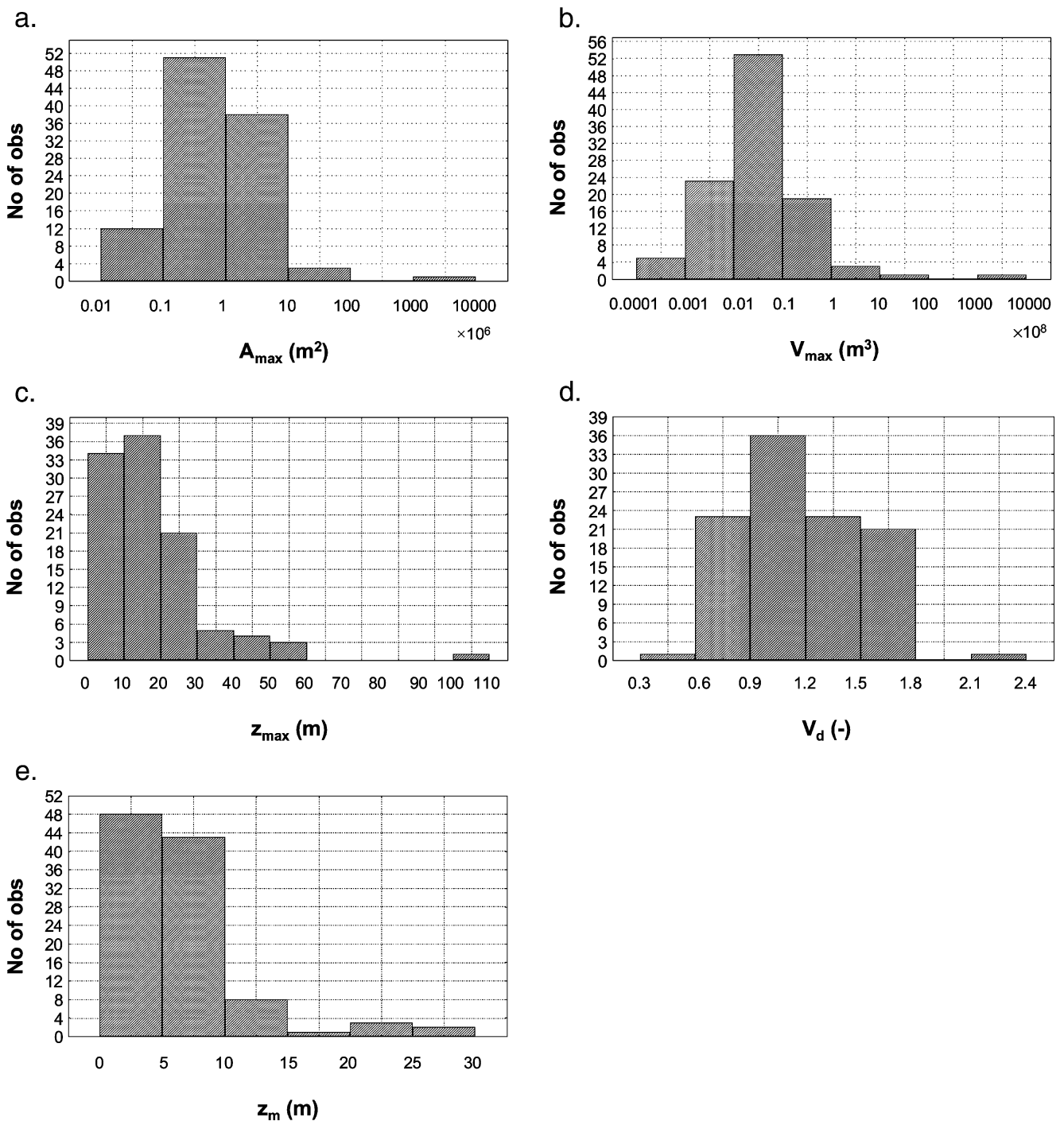


**Fig. 5** Histograms of morphometric characteristics of the lakes used in this work. (a) Surface area ( $A_{max}$ ), (b) volume ( $V_{max}$ ), (c) maximum depth ( $z_{max}$ ), (d) volume development parameter ( $V_d=(3z_m/z_{max})$ ) and (e) mean depth ( $z_m=V/A$ ). Data from 105 lakes

summarised in Fig. 5. They originate from Anderson [1], Andersson et al. [2], Bengtsson et al. [3], Bodbacka Fältman [6], Elert et al. [13], Grahn et al. [18], Henrikson and Nyman [37], Henrikson et al. [38], Håkanson [20] (and references therein), Jansson [45, 46], Persson (personal communication) and Rhode [67]. Areas and volumes for

these lakes range from about  $1.7 \times 10^4$  to  $5.6 \times 10^9$   $m^2$  and  $2.1 \times 10^4$  to  $1.5 \times 10^{11}$   $m^3$ , respectively; the maximal depths range between 2 and 106 m. Compared to the variation in  $V_d$  (0.33–2.30) in Neumann’s study [58], these lakes range from 0.54 to 2.42 with an average of 1.19 compared to Neumann’s 1.40.

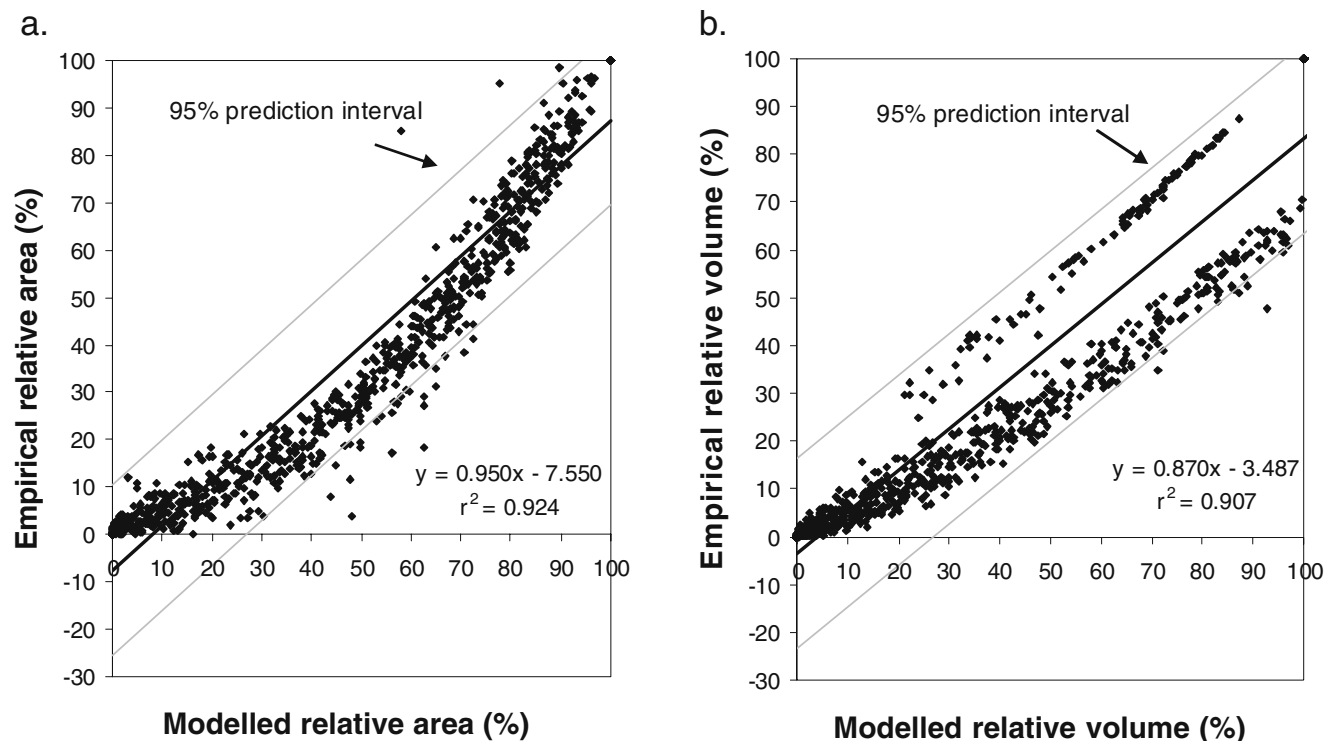


**Fig. 6** Comparisons of values estimated from the  $V_d$  approach and empirical values, including the resulting 95% prediction interval. (a) Relative area. (b) Relative volume. Based on data from 105 area–depth and volume–depth distribution curves

## 4 Results

### 4.1 Estimations Based on the Volume Development and Comparisons with Empirical Data

#### 4.1.1 Area–depth Distribution Curves

Figure 6a shows that the approximation based on  $V_d$  estimates the area quite well. Analysis of the residuals gives a 95% confidence interval for individual values, i.e., the prediction interval, of  $\pm 17.9\%$  in the units of the estimated value. The confidence interval for individual predicted values gives the range of values within which an additional observation of the predicted variable can be expected to be located with a 95% level of certainty. The coefficient of determination ( $r^2$ ) is 0.924 (see Table 2). The slope and the intercept of the regression line are 0.950 and  $-7.550$ , respectively. This indicates that the approach gives an overestimation in many cases.

A regression analysis was also carried out without the endpoints, i.e., relative areas 0% and 100%, to study the influence of these values. Since the endpoints always are modelled correctly, there is a risk that these values will influence the results. However, excluding the endpoints only alters the regression equation and  $r^2$  slightly (Table 2).

#### 4.1.2 Volume–depth Distribution Curves

The volumes estimated with the Simpson approximation (equation (5)) and the linear approximation (equation (6)) were first compared to the “more exact” volume approximation, introduced in Section 2.3.1, of the area–depth distribution curves generated by the  $V_d$ -approach. To determine which of these equations gives the best volume estimations for different  $V_d$ -values and at different relative depths, their relative errors, calculated as  $100|V_{\text{more exact}} - V_{\text{estimated}}|/V_{\text{more exact}}$ , were compared. The relative errors in the volumes calculated using the Simpson approximation and the linear approximation could then be compared to determine the intervals in  $V_d$  and relative depth where one or the other approximation estimates the volume most accurately. Results are summarised in Fig. 7 (see Appendix for more details about the specific intervals). In Fig. 7, it can be noted that the linear approximation (equation (6)) is generally best at very small, relative depths as well as towards greater depths in lakes with a somewhat concave basin shape, i.e., when approximately  $1.5 < V_d < 2.5$ , whereas the Simpson approximation gives better results at the opposite relative depths and  $V_d$ -values. Using the different volume formulas within the recommended limits in Fig. 7 thereby gives the smallest possible errors.

**Table 2** Slope, intercept, number of observations (*n*) and *r*<sup>2</sup>-value for the regression line between empirical and estimated relative areas from the *V*<sub>d</sub>-approach with and without endpoints (i.e., 0% and 100%)

Model	Endpoints	Slope	Intercept	<i>n</i>	<i>r</i> <sup>2</sup>
Relative area	Yes	0.950	-7.550	1,007	0.924
Relative area	No	0.903	-7.985	797	0.913

Using the different volume formulas recommended in Fig. 7, we compared estimated volumes with empirical ones (see Fig. 6b). The *r*<sup>2</sup> is 0.907 and the 95% prediction interval is ±19.9% in units of the estimated value. The slope and the intercept of the regression line are 0.870 and -3.487, respectively, and indicate that the model mostly gives an overestimation. In this case, exclusion of the endpoints only alters the regression moderately (see Table 3).

#### 4.2 Estimations Based on the Hypsographic Development Parameter and Comparisons with Empirical Data

##### 4.2.1 Area–depth Distribution Curves and Volume–depth Distribution Curves

Comparisons between calculated relative areas and volumes and empirical data in Fig. 8 show that the *H*<sub>d</sub>-approach gives both the relative area (equation (10)) and, in particular, the relative volume (equation (13)), with a very high accuracy. For each lake, *H*<sub>d</sub> has been estimated by recalculating of the empirical *V*<sub>d</sub>-value through equations (15)–(18).

Regression analysis in Fig. 8 gives information about the interval within which it is expected that 95% of all data points fall for an individual estimation. For the relative area and volume, it is expected that individual estimations with a 95% level of certainty would fall ±7.0% and ±3.2% in units of the estimated value, respectively, from the respective

**Table 3** Slope, intercept, number of observations (*n*) and *r*<sup>2</sup>-value for the regression line between empirical and estimated relative volumes from the *V*<sub>d</sub>-approach with and without endpoints (i.e., 0% and 100%)

Model	Endpoints	Slope	Intercept	<i>n</i>	<i>r</i> <sup>2</sup>
Relative volume	Yes	0.870	-3.487	1,007	0.907
Relative volume	No	0.735	-1.573	797	0.884

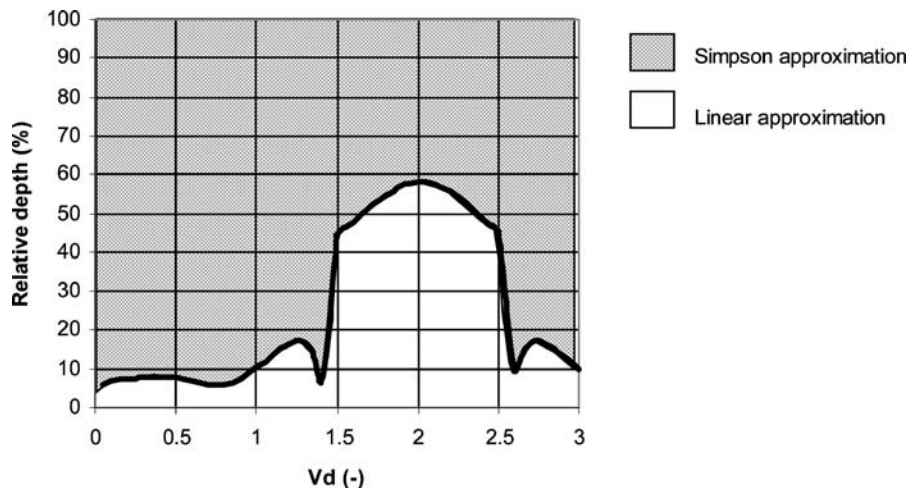
regression line. The *r*<sup>2</sup>-values for relative area and relative volume estimations are 0.988 and 0.996, respectively (see Table 4). Since the slopes and intercepts of both models are very close to 1 and 0, respectively, these models give estimations with very small deviations from empirical values. As with the *V*<sub>d</sub>-approach, we examined how exclusions of the endpoints alter the *r*<sup>2</sup>-values, slopes and intercepts of the regression lines. The changes are very small (see Table 4).

#### 4.3 Correction Factor for Volume Determinations

In Section 3.1, we introduced an approach to identify and omit lakes whose empirical volumes cannot be determined with satisfactory accuracy. To determine if and when it is a necessity to make corrections, we generated idealised area–depth distribution curves with known volumes by means of the *H*<sub>d</sub>-approach (equation (10)). Volumes of *H*<sub>d</sub>-derived lake bodies (*V*<sub>true</sub>) were compared to volume estimations (*V*<sub>linear</sub>) from the linear volume formula (equation (2)) for different basin shapes and numbers of strata. Results are visualised in Fig. 9 in terms of a correction factor (*C*<sub>f</sub>=*V*<sub>true</sub>/*V*<sub>linear</sub>) that represents the values with which empirical, linearly estimated, volumes should be multiplied to yield more correct volumes.

These results can be summarised in a few equations. However, due to statistical limitations and practical reasons,

**Fig. 7** An illustration showing which model (Simpson approximation or linear volume approximation) gives the best volume estimations of the “more exact” volume of the area–depth distribution curves generated by the *V*<sub>d</sub>-approach. The different patterns indicate which of the two models, for the given combinations of relative depth and *V*<sub>d</sub>-values, gives the best volume estimation



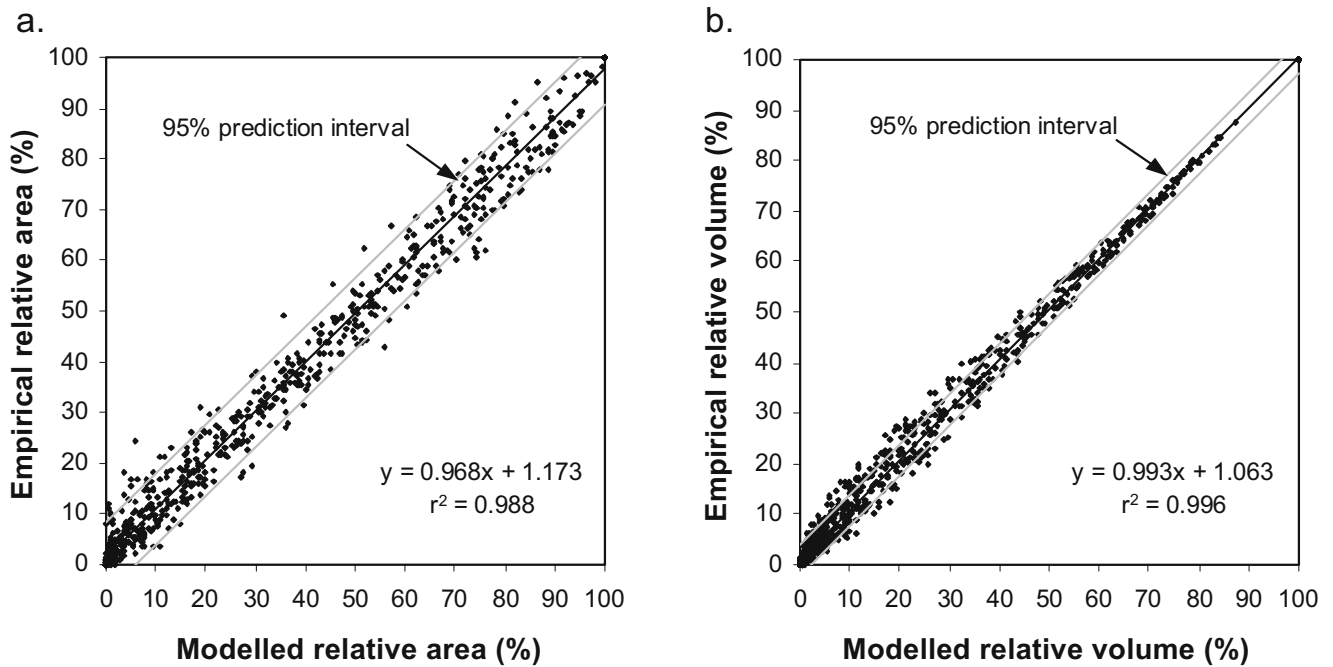


**Fig. 8** A comparison between empirical and modelled values for area and volume from the  $H_d$ -approach, including the resulting 95% prediction interval for individual estimations. (a) Relative area. (b) Relative volume. Based on data from 105 area- and volume-depth distribution curves

these equations were only derived for cases when the number of strata equals five or more and when  $C_f$ -values deviate more than 0.5% from the ideal value of one. To estimate  $C_f$  for empirical, linearly estimated  $V_d$ -values in the range 0.35–2.75, the following equations were derived:

$$C_f = 1 / 10^{(-3.06 \log(V_d) - 2.03 \log(\text{Strata}) + 0.29 \log(V_d) \log(\text{Strata}) - 0.69)} \quad (19)$$

$(0.35 \leq V_d < 1.46 \text{ and } 5 \leq \text{Strata} \leq 35)$

$$C_f = 10^{(5.48V_d + 0.57\text{Strata} - 0.32V_d\text{Strata} - 14.87)} \quad (20)$$

$(2.38 < V_d \leq 2.75 \text{ and } 5 \leq \text{Strata} \leq 9)$

**Table 4** Slopes, intercepts, number of observations ( $n$ ) and  $r^2$  for the regressions between empirical and estimated relative areas and relative volumes from the  $H_d$ -approach with and without endpoints (i.e., 0% and 100%)

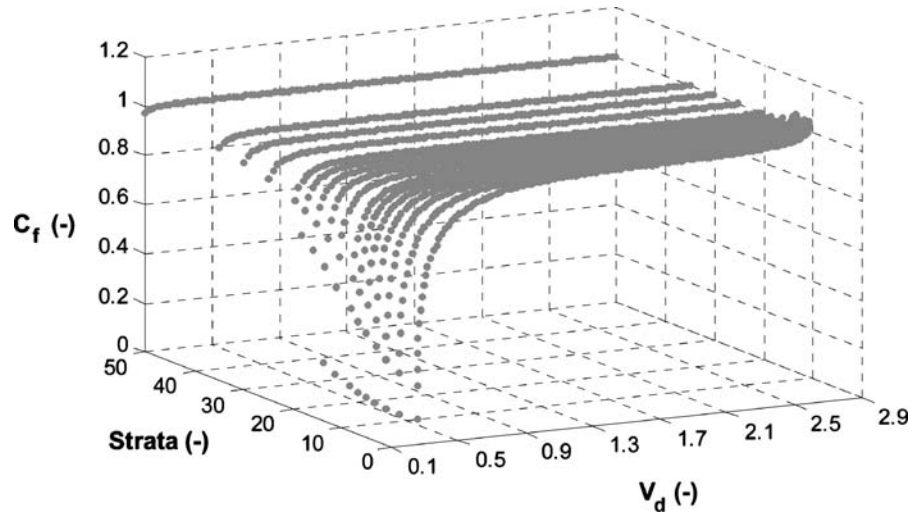
Model	Endpoints	Slope	Intercept	$n$	$r^2$
Relative area	Yes	0.968	1.173	1,007	0.988
Relative area	No	0.948	1.715	797	0.908
Relative volume	Yes	0.993	1.063	1,007	0.996
Relative volume	No	0.994	1.228	797	0.991

where  $V_d$  is the empirical volume development factor for which the volume has been determined with the linear volume calculation formula (equation (2)) and Strata is the number of existing strata on the corresponding bathymetric map. Note that given empirical  $V_d$ -ranges for the equations represent  $V_d$ -values that after correction with  $C_f$  include 0.33 and 2.70, i.e., the lower and upper boundaries for the worldwide range of  $V_d$ -values identified in this work. A comparison of estimated  $C_f$ -values from equations (19) and (20) to correct  $C_f$ -values (i.e.,  $C_f = V_{\text{true}}/V_{\text{linear}}$ ) shows that these equations can be used to successfully estimate  $C_f$  for the given ranges of  $V_d$  and strata. The deviation in percent between estimated and correct  $C_f$ , defined as  $100|C_{f, \text{correct}} - C_{f, \text{estimated}}|/C_{f, \text{correct}}$ , increases the more the correct  $C_f$ -value deviates from the ideal value of 1. For equation (19), the deviation is  $\sim 0.03\%$  for  $C_f = \sim 0.998$ , whereas the deviation is  $\sim 3.2\%$  for  $C_f = \sim 0.75$ . For equation (20), the deviation is  $\sim 0.05\%$  for  $C_f = \sim 1.002$ , whereas the deviation is  $\sim 3.7\%$  for  $C_f = \sim 1.11$ . Our findings further indicate that

**Table 5** Mean depth ( $z_m$ ), maximum depth ( $z_{\text{max}}$ ), surface area ( $A_{\text{max}}$ ), maximum volume ( $V_{\text{max}}$ ), change in water level ( $z$ ), relative depth of the new lake level ( $z_{\text{rel}} = z/z_{\text{max}}$ ) and volume development ( $V_d$ ) in Lake Kinneret (modified from Håkanson et al. [31])

$z_m$ (m)	$z_{\text{max}}$ (m)	$A_{\text{max}}$ ( $\text{m}^2$ )	$V_{\text{max}} = z_m A_{\text{max}}$ ( $\text{m}^3$ )	$z$ (m)	$z_{\text{rel}}$ (%)	$V_d = 3z_m/z_{\text{max}}$ (-)
26	42	$170 \times 10^6$	$442 \times 10^7$	4.0	9.5	1.86

**Fig. 9** An illustration of how the magnitude of the correction factor ( $C_f$ ) deviates from the ideal value of 1, as a function of differences in lake basin shapes ( $V_d=0.10-2.90$ ) and number of existing strata ( $n=4-50$ ) in lake bathymetric maps



there is no need to correct empirical volumes determined with the linear approximation formula (equation (2)) in the following cases, (a)  $V_d=0.35-1.46$  and  $Strata>35$ , (b)  $V_d=1.46-2.38$  and  $Strata\geq 5$ , and (c)  $V_d=2.38-2.75$  and  $Strata>9$ .

**5 Example of Practical Use**

Assume that we want to calculate the new surface area and volume of Lake Kinneret for the dry season (July–September) when water level is lowered by 4 m. The mean depth, maximum depth and surface area of Lake Kinneret can be found in Håkanson et al. [31], and from these values, the maximum volume and the volume development parameter can be calculated (see Table 5). We then have all the variables needed to calculate the new area and volume using either of the two approaches introduced in this work.

**5.1 The  $V_d$ -approach**

With the  $V_d$ -approach, the new surface area corresponding to a water level change of 4 m is calculated from equation (3). We then use the information in Fig. 7 to determine which approximation to use for the volume calculation. For

a relative depth of 9.5% and a volume development parameter of 1.86, one finds that the linear approximation (i.e., equation (6)) should be used. The new volume from equation (6) and the new surface area are given Table 6. The 95% prediction intervals for this approach, 17.9% for area and 19.9% for volume, correspond to  $30.4 \times 10^6$  m<sup>2</sup> ( $0.179A_{max}$ ) and  $88.0 \times 10^7$  m<sup>3</sup> ( $0.199V_{max}$ ).

**5.2 The  $H_d$ -approach**

We begin by calculating  $H_d$  from equations (15)–(18). Since  $V_d$  in this case is 1.86, we use equation (17) and derive a  $H_d$  of 0.0326. The new surface area corresponding to a water level change of 4 m is then calculated from equation (10). Finally, by putting  $z_i$  to 4 m and  $z_{i+1}$  to 42 m in equation (13), the new volume is obtained. The resulting area and volume are given in Table 6. Here, the 95% prediction intervals of 7.0% for area and 3.2% for volume correspond to  $11.9 \times 10^6$  m<sup>2</sup> ( $0.070A_{max}$ ) and  $14.1 \times 10^7$  m<sup>3</sup> ( $0.032V_{max}$ ).

**6 Discussion and Conclusions**

The models presented in this work are meant to provide a morphometric basis for the development of ecosystem models that are capable of describing the vertical extension of physical processes and associated chemical, biological and physical properties important to lake ecosystems. We have developed two new approaches to mathematically describe differences in basin shapes both among and within lakes. The similarity between the two approaches is that they are based on volume, surface area and maximum depth. The first model is derived from the volume

**Table 6** Results from applying the  $V_d$ - and  $H_d$ -approaches to Lake Kinneret. Area corresponding to a water level change of 4 m,  $A$  ( $z=4$  m), and volume below 4 m depth,  $V$  ( $z=4$  m)

Method	$A$ ( $z=4$ m) (m <sup>2</sup> )	$V$ ( $z=4$ m) (m <sup>3</sup> )
$V_d$ -approach	$165 \times 10^6$	$375 \times 10^7$
$H_d$ -approach	$166 \times 10^6$	$376 \times 10^7$

development ( $V_d$ ) and the second model from a new morphometric parameter, the hypsographic development parameter ( $H_d$ ). Both models give quite good correlation both for area and volume when compared to empirical data, although the  $H_d$ -model gives more accurate and precise estimations. The evaluations of the two approaches were made using lakes with  $V_d$ -values in the range 0.54–2.42 and are therefore only valid within these ranges. However, the models are meant to be applied to all lakes, although most of the lakes used in testing the approaches in this work are of glacial origin, most lakes on earth belong to the glacial type as well and the given range of  $V_d$ -values cover a large portion of the existing range of  $V_d$ -values in the world.

With the  $H_d$ -model, any individual estimation of area and volume at any depth in a lake would, with a 95% level of certainty, fall within  $\pm 7.0\%$  and  $\pm 3.2\%$ , in the units of the estimated value, respectively, from respective regression line for empirical versus modelled data. Estimations from the  $V_d$ -approach, on the other hand, are easier to derive and

can be used when tolerance to deviations is greater, e.g., in models not so sensitive to errors in area and volume. For the  $V_d$ -model, it can be expected with a 95% level of certainty that any individual estimation of area and volume would fall  $\pm 17.9\%$  and  $\pm 19.9\%$  in the units of the estimated value, respectively, from respective regression line.

Recognising that both the  $V_d$ - and especially the  $H_d$ -approach describe the lake form quite well, it is expected that the bottom slope formulas presented in this work would also prove to be useful.

We were further able to use the  $H_d$ -model to determine when it is necessary to revise the empirical volume of a lake. In these cases, the derived equations, based on the number of strata and information on basin shapes ( $V_d$ ), can be used to estimate the correct volume.

**Acknowledgements** We would like to express our gratitude to Gunnar Persson at the Swedish University of Agricultural Sciences for giving us access to several unpublished lake hypsographic curves from a database maintained by the Department of Environmental Assessment.

## Appendix

**Table 7** Limits in  $V_d$  and relative depth within which the Simpson approximation (equation (5)) or the linear approximation (equation (6)) is recommended for calculations of the volume below the relative depth in question

$V_d$	Recom. approx. below limit	Limit (relative depth)	Recom. approx. above limit	$V_d$	Recom. approx. below limit	Limit (relative depth)	Recom. approx. above limit	$V_d$	Recom. approx. below limit	Limit (relative depth)	Recom. approx. above limit
0.05	Linear	0.057	Simpson	1.05	Linear	0.120	Simpson	2.05	Linear	0.579	Simpson
0.1	Linear	0.071	Simpson	1.1	Linear	0.136	Simpson	2.1	Linear	0.575	Simpson
0.15	Linear	0.073	Simpson	1.15	Linear	0.152	Simpson	2.15	Linear	0.567	Simpson
0.2	Linear	0.074	Simpson	1.2	Linear	0.165	Simpson	2.2	Linear	0.556	Simpson
0.25	Linear	0.076	Simpson	1.25	Linear	0.172	Simpson	2.25	Linear	0.542	Simpson
0.3	Linear	0.079	Simpson	1.3	Linear	0.169	Simpson	2.3	Linear	0.525	Simpson
0.35	Linear	0.080	Simpson	1.35	Linear	0.145	Simpson	2.35	Linear	0.507	Simpson
0.4	Linear	0.081	Simpson	1.4	Linear	0.066	Simpson	2.4	Linear	0.488	Simpson
0.45	Linear	0.08	Simpson	1.45	Linear	0.196	Simpson	2.45	Linear	0.470	Simpson
0.5	Linear	0.078	Simpson	1.5	Linear	0.447	Simpson	2.5	Linear	0.453	Simpson
0.55	Linear	0.075	Simpson	1.55	Linear	0.461	Simpson	2.55	Linear	0.247	Simpson
0.6	Linear	0.070	Simpson	1.6	Linear	0.478	Simpson	2.6	Linear	0.099	Simpson
0.65	Linear	0.066	Simpson	1.65	Linear	0.496	Simpson	2.65	Linear	0.135	Simpson
0.7	Linear	0.061	Simpson	1.7	Linear	0.513	Simpson	2.7	Linear	0.167	Simpson
0.75	Linear	0.059	Simpson	1.75	Linear	0.530	Simpson	2.75	Linear	0.172	Simpson
0.8	Linear	0.060	Simpson	1.8	Linear	0.546	Simpson	2.8	Linear	0.164	Simpson
0.85	Linear	0.065	Simpson	1.85	Linear	0.559	Simpson	2.85	Linear	0.151	Simpson
0.9	Linear	0.075	Simpson	1.9	Linear	0.569	Simpson	2.9	Linear	0.134	Simpson
0.95	Linear	0.088	Simpson	1.95	Linear	0.576	Simpson	2.95	Linear	0.116	Simpson
1	Linear	0.103	Simpson	2	Linear	0.579	Simpson	3	Linear	0.099	Simpson

## References

1. Anderson, C. (1997). Limnologisk undersökning av Lötsjön, april–augusti 1996. *Scripta Limnologica Upsaliensia 1997, B:4*, 47 (in Swedish).
2. Andersson, P., Borg, H., Holmgren, K., & Håkanson, L. (1987). *Typsjöar och tillrinningsområden i projektet kalkning-kviksilver vid naturvårdsverkets PU-Lab, SNV Rapport 3396* (p. 80) (in Swedish).
3. Bengtsson, Å., Viklund, T., Häggblom, M., Andersson, T., & Håkanson, L. (1987). *Typsjöar och tillrinningsområden i Västernorrlands län, SNV Rapport 3402* (p. 81) (in Swedish).
4. Blais, J. M., & Kalff, J. (1995). The influence of lake morphometry on sediment focusing. *Limnology and Oceanography*, *40*, 582–588.
5. Blom, G., van Duin, E. H. S., & Lijklema, L. (1994). Sediment resuspension and light conditions in some shallow Dutch lakes. *Water Science and Technology*, *30*, 243–252.
6. Bodbacka Fältman, L. (1991). *Sedimentary structures and sediment accumulation in the lakes lilla Ullfjärden and stora Ullfjärden, studied by the X-ray radiographic technique, UNGI Rapport 83*. Uppsala University, Institute of Earth Sciences, Physical Geography (p. 113).
7. Charlton, M. N. (1980). Hypolimnion oxygen consumption in lakes: Discussion of productivity and morphometry effects. *Canadian Journal of Fisheries and Aquatic Sciences*, *37*, 1531–1539.
8. Cole, J. J., & Pace, M. L. (1998). Hydrological variability of small northern Michigan lakes measured by the addition of tracers. *Ecosystems*, *1*, 310–320.
9. Cornett, R. J. (1989). Predicting changes in hypolimnetic oxygen concentrations with phosphorus retention, temperature, and morphometry. *Limnology and Oceanography*, *34*, 1359–1366.
10. Cornett, R. J., & Rigler, F. H. (1987). Vertical transport of oxygen into the hypolimnion of lakes. *Canadian Journal of Fisheries and Aquatic Sciences*, *44*, 852–858.
11. Crapper, P. F., Fleming, P. M., & Kalma, J. D. (1996). Prediction of lake levels using water balance models. *Environmental Software*, *11*, 251–258.
12. Duarte, C. M., & Kalff, J. (1986). Littoral slope as a predictor of the maximum biomass of submerged macrophyte communities. *Limnology and Oceanography*, *31*, 1072–1080.
13. Elert, M., Meili, M., Östlund, M., & Johansson, J.-Å. (1998). *Kviksilver i Rolfstaån - Delångersån, undersökningar och modelleringar av ackumulering och transport, SNV Rapport 4868* (p. 68) (in Swedish).
14. Fee, E. J. (1979). A relation between lake morphometry and primary productivity and its use in interpreting whole-lake eutrophication experiments. *Limnology and Oceanography*, *24*, 401–416.
15. Fee, E. J., Hecky, R. E., Kasian, S. E. M., & Cruikshank, D. R. (1996). Effects of lake size, water clarity, and climatic variability, on mixing depths in Canadian Shield lakes. *Limnology and Oceanography*, *41*, 912–920.
16. Gibson, C. E., & Guillot, J. (1997). Sedimentation in a large lake: The importance of fluctuations in water level. *Freshwater Biology*, *37*, 597–604.
17. Goodchild, M. F., Steyaert, L. T., Parks, B. O., Johnston, C., Maidment, D., Crane, M., et al. (1996). *GIS and environmental modeling: Progress and research issues*. Fort Collins, CO: GIS World Books.
18. Grahn, P., Thorssell, S., Nilsson, Å., & Håkanson, L. (1987). *Typsjöar och tillrinningsområden i Örebro län, SNV Rapport 3384* (p. 83) (in Swedish).
19. Ha, S. R., Bae, G. J., Park, D. H., & Cho, J. H. (2003). Improvement of pre- and post-processing environments of the dynamic two-dimensional reservoir model CE-QUAL-W2 based on GIS. *Water Science and Technology*, *48*, 79–88.
20. Håkanson, L. (1977). On lake form, lake volume and lake hypsographic survey. *Geografiska Annaler A*, *59*, 1–29.
21. Håkanson, L. (1977). The influence of wind, fetch, and water depth on the distribution of sediments in Lake Vänern, Sweden. *Canadian Journal of Earth Sciences*, *14*, 397–412.
22. Håkanson, L. (1981). *A manual of lake morphometry*. Berlin, Heidelberg, New York: Springer-Verlag.
23. Håkanson, L. (1981). Determination of characteristic values for physical and chemical lake sediment parameters. *Water Resources Research*, *17*, 1625–1640.
24. Håkanson, L. (1981). On lake bottom dynamics – the energy–topography factor. *Canadian Journal of Earth Sciences*, *18*, 899–909.
25. Håkanson, L. (1982). Lake bottom dynamics and morphometry – the dynamic ratio. *Water Resources Research*, *18*, 1444–1450.
26. Håkanson, L. (1994). How many lakes are there in Sweden? *Geografiska Annaler A*, *76*, 203–205.
27. Håkanson, L. (1997). Testing different sub-models for the partition coefficient and the retention rate for radicesium in lake ecosystem modelling. *Ecological Modelling*, *101*, 229–250.
28. Håkanson, L. (1999). *Water pollution – methods and criteria to rank, model and remediate chemical threats to aquatic ecosystems*. Leiden: Backhuys Publishers.
29. Håkanson, L. (2000). The role of characteristic coefficients of variation in uncertainty and sensitivity analyses, with examples related to the structuring of lake eutrophication models. *Ecological Modelling*, *131*, 1–20.
30. Håkanson, L. (2005). The importance of lake morphometry for the structure and function of lakes. *International Review of Hydrobiology*, *90*, 433–461.
31. Håkanson, L., Parparov, A., & Hambricht, K. D. (2000). Modelling the impact of water level fluctuations on water quality (suspended particulate matter) in Lake Kinneret, Israel. *Ecological Modelling*, *128*, 101–125.
32. Håkanson, L., & Peters, R. H. (1995). *Predictive limnology – methods for predictive modelling*. Amsterdam: SPB Academic Publishing.
33. Hamilton, D. P., & Mitchell, S. F. (1996). An empirical model for sediment resuspension in shallow lakes. *Hydrobiologia*, *317*, 209–220.
34. Hamilton, D. P., & Mitchell, S. F. (1997). Wave-induced shear stresses, plant nutrients and chlorophyll in seven shallow lakes. *Freshwater Biology*, *38*, 159–168.
35. Hanna, M. (1990). Evaluation of models predicting mixing depth. *Canadian Journal of Fisheries and Aquatic Sciences*, *47*, 940–947.
36. Hellström, T. (1991). The effect of resuspension on algal production in a shallow lake. *Hydrobiologia*, *213*, 183–190.
37. Henriksson, L., & Nyman, H. G. (1992). Mjörn - En limnologisk studie 1990. *Länsstyrelsen Älvsborgs Län, 1992(4)*, 107 pp. (in Swedish).
38. Henriksson, L., Nyman, H. G., & Oscarson, H. G. (1987). Lyngern - 1984 och för hundra år sedan, Länsstyrelsen Älvsborgs län 1987:1 & länsstyrelsen Hallands län 1987:1, 133 pp. (in Swedish).
39. Henson, E. B. (1993). Estimating the areal extent of the littoral zone in lakes. *Verhandlungen Internationale Vereinigung Limnologie*, *25*, 414–418.
40. Hilton, J., Lishman, J. P., & Allen, P. V. (1986). The dominant processes of sediment distribution and focusing in a small, eutrophic, monomictic lake. *Limnology and Oceanography*, *31*, 125–133.
41. Home, A. J., & Goldman, C. R. (1994) *Limnology*. Singapore: McGraw-Hill.
42. Imboden, D. M. (1973). Limnologische transport- und Nährstoff-

- modelle. *Schweizerische Zeitschrift für Hydrologie*, 35, 29–68 (in German).
43. James, W. F., & Barko, J. W. (1993). Sediment resuspension, redeposition, and focusing in a small dimictic reservoir. *Canadian Journal of Fisheries and Aquatic Sciences*, 50, 1023–1028.
  44. James, R. T., Martin, J., Wool, T., & Wang, P. F. (1997). A sediment resuspension and water quality model of Lake Okeechobee. *Journal of the American Water Resources Association*, 33, 661–680.
  45. Jansson, M. (1977). Vattenbalans och kemiska budgetberäkningar för Stugsjön 1971–1975. In *Experiment med gödning av sjöar i Kuokkelområdet, Kuokkelprojektets rapport Nr. 5* (pp. 3–42). Uppsala: Uppsala universitet, Limnologiska institutionen (in Swedish).
  46. Jansson, M. (1978). Abiotiska förhållanden i Gunillajaurer 1977. In *Sjögödslingsexperiment i Kuokkelområdet, Kuokkelprojektets rapport Nr. 6* (pp. 5–24). Uppsala: Uppsala universitet, Limnologiska institutionen (in Swedish).
  47. Johansson, H., Lindström, M., & Håkanson, L. (2001). On the modelling of the particulate and dissolved fractions of substances in aquatic ecosystems – sedimentological and ecological interactions. *Ecological Modelling*, 137, 225–240.
  48. Johnson, T. C. (1980). Sediment redistribution by waves in lakes, reservoirs and embayments. In H. G. Stefan (Ed.), *Proceedings of the symposium on surface water impoundments*, June 2–5, 1980, Minneapolis, Minnesota (pp. 1307–1317). USA: American Society of Civil Engineers.
  49. Kalchew, R., Botev, I., Hristozova, M., Naidenow, W., Raikova-Petrova, G., Stoyneva, M., et al. (2004). Ecological relations and temporal changes in the pelagial of the high mountain lakes in the Rila Mountains (Bulgaria). *Journal of Limnology*, 63, 90–100.
  50. Konitzer, K. (1999). Redistribution of Chernobyl <sup>137</sup>Cs in lake sediment, Licentiate thesis, Uppsala University, Uppsala, Sweden.
  51. Kuo, J. T., & Wu, J. H. (1991). A nutrient model for a lake with time-variable volumes. *Water Science and Technology*, 24, 133–139.
  52. Lind, O. T., Chrzanowski, T. H., & Dávalos-Lind, L. (1997). Clay turbidity and the relative production of bacterioplankton and phytoplankton. *Hydrobiologia*, 353, 1–18.
  53. Lind, O. T., Dávalos-Lind, L. O., Chrzanowski, T. H., & Limón, J. G. (1994). Inorganic turbidity and the failure of fishery models. *Internationale Revue der Gesamten Hydrobiologie*, 79, 7–16.
  54. Lindström, M., Håkanson, L., Abrahamsson, O., & Johansson, H. (1999). An empirical model for prediction of lake water suspended particulate matter. *Ecological Modelling*, 121, 185–198.
  55. Meybeck, M. (1995). Global distribution of lakes. In A. Lerman, D. M. Imboden & J. R. Gat (Eds.), *Physics and chemistry of lakes* (pp. 1–32). Heidelberg, New York: Springer Verlag.
  56. Molot, L. A., Dillon, P. J., Clark, B. J., & Neary, B. P. (1992). Predicting end-of-summer oxygen profiles in stratified lakes. *Canadian Journal of Fisheries and Aquatic Sciences*, 49, 2363–2372.
  57. Naoum, S., Tsanis, I. K., & Fullarton, M. (2005). A GIS pre-processor for pollutant transport modelling. *Environmental Modelling & Software*, 20, 55–68.
  58. Neumann, J. (1959). Maximum depth and average depth of lakes. *Journal of the Fisheries Research Board of Canada*, 16, 923–927.
  59. Nöges, P., Tuvikene, L., Nöges, T., & Kisand, A. (1999). Primary production, sedimentation and resuspension in large shallow Lake Võrtsjärv. *Aquatic Sciences*, 61, 168–182.
  60. Parparov, A., & Hambright, K. D. (1996) A proposed framework for the management of water quality in arid-region lakes. *Internationale Revue der Gesamten Hydrobiologie*, 81, 435–454.
  61. Patalas, K. (1984). Mid-summer mixing depths of lakes of different latitudes. *Verhandlungen Internationale Vereinigung Limnologie*, 22, 97–102.
  62. Rasmussen, J. B. (1988). Littoral zoobenthic biomass in lakes, and its relationship to physical, chemical, and trophic factors. *Canadian Journal of Fisheries and Aquatic Sciences*, 45, 1436–1447.
  63. Rasmussen, J. B., Godbout, L., & Schallenberg, M. (1989). The humic content of lake water and its relationship to watershed and lake morphometry. *Limnology and Oceanography*, 34, 1336–1343.
  64. Rawson, D. S. (1952). Mean depth and the fish production of large lakes. *Ecology*, 33, 513–521.
  65. Rawson, D. S. (1955). Morphometry as a dominant factor in the productivity of large lakes. *Verhandlungen Internationale Vereinigung Limnologie*, 12, 164–175.
  66. Rempel, R. S., & Colby, C. J. (1991). A statistically valid model of the morphoedaphic index. *Canadian Journal of Fisheries and Aquatic Sciences*, 48, 1937–1943.
  67. Rhode, A. (1972). Termiska studier i sjöar i Kassjöans representativa område, 3-betygsuppsats i hydrologi, naturgeografiska institutionen, avdelningen för hydrologi. Uppsala: Uppsala universitet (in Swedish).
  68. Rowan, D. J., Kalf, J., & Rasmussen, J. B. (1992). Estimating the mud deposition boundary depth in lakes from wave theory. *Canadian Journal of Fisheries and Aquatic Sciences*, 49, 2490–2497.
  69. Schallenberg, M., James, M., Hawes, I., & Howard-Williams, C. (1999). External forcing by wind and turbid inflows on a deep glacial lake and implications for primary production. *New Zealand Journal of Marine Freshwater Research*, 33, 311–331.
  70. Walker, W. W. (1979). Use of hypolimnetic oxygen depletion rate as a trophic state index for lakes. *Water Resources Research*, 15, 1463–1470.
  71. Wetzel, R. G. (1983). *Limnology*. Philadelphia: Saunders College Publishing.
  72. Weyhenmeyer, G. A. (1996). The significance of lake resuspension in lakes. PhD thesis, Uppsala University, Uppsala, Sweden.